Domestic Animal Endocrinology 95 (2026) 106998

Contents lists available at ScienceDirect

Domestic Animal Endocrinology

journal homepage: www.journals.elsevier.com/domestic-animal-endocrinology

# Pancreatic islet remodeling in horses with hyperinsulinemia and pituitary dysfunction

P. Teague *, M. Dark, D. Verdugo, D. Freeman, D. McFarlane

*University of Florida College of Veterinary Medicine, 2015 SW 16th Street Gainesville, FL, United States*

ARTICLE INFO

*Keywords:*
Pancreas
Islets
Insulin
Hyperinsulinemia
Horse

ABSTRACT

The equine pancreas remains understudied, particularly in the context of endocrine disease. This study aimed to characterize regional islet distribution and composition in the normal equine pancreas and investigate how hyperinsulinemia (HI) and pituitary pars intermedia dysfunction (PPID) influence pancreatic islet morphology and hormone expression. In the first experiment, pancreas samples from eight healthy horses were collected and analyzed across three anatomical locations: left lobe, body, and right lobe. The left lobe exhibited a greater relative islet area and perimeter compared to the body and right lobe, though islet composition remained consistent with a similarly proportional alpha-cell core, beta-cell mantle, and scattered delta-cells. In the second experiment, pancreas tissues from thirty-five horses with defined endocrine disease status were evaluated. HI was associated with larger islets and greater insulin immunostaining, while PPID was associated with increased islet number without changes in islet size or insulin immunostaining, suggesting divergent disease-specific adaptations. Findings support the hypothesis that HI drives islet expansion as a compensatory response to insulin resistance, whereas PPID promotes islet neogenesis. The observed increase in islet number in PPID horses may reflect a previously unrecognized mechanism influenced by chronic endocrine stimulation. These results established foundational knowledge of normal equine islet architecture and highlight the dynamic adaptability of the endocrine pancreas in response to metabolic and pituitary disorders.

## 1. Introduction

The equine pancreas remains relatively understudied, particularly in endocrine disease. A better understanding of equine endocrine pancreatic anatomy including cellular distribution, composition, and function is necessary to provide a basis for strategic sampling for designing future studies. Earlier investigations into the equine endocrine pancreas unveiled a distinctive islet composition in horses compared to other species [1,2]. While other species such as rodents, cats, and dogs exhibit a beta-cell core and an alpha-cell periphery with sporadic distribution of delta- and pancreatic polypeptide-cells (PP-cells), horses display an alpha-cell core and a beta-cell periphery, with similar sporadic distribution of delta- and PP-cells within the islets. This unique islet composition was first identified in 1976 and remained unexplored until 1989 when Furuoka and colleagues not only affirmed the previous findings but also explored the distribution and composition of islets throughout the equine pancreas, revealing a smaller diameter of islets in the right lobe compared to the left lobe [3,2]. More recent studies compared hormone expression of endocrine cells in normal versus metabolically diseased horses, which also reaffirmed the equine islet's distinctive composition [4].

Equine metabolic syndrome (EMS) is a collection of risk factors that predisposes horses to the development of laminitis, a painful condition of the hoof. These risk factors include increased regional or general adiposity, insulin dysregulation (ID) characterized by baseline or postprandial hyperinsulinemia (HI), and a predisposition toward laminitis [5]. The term ID collectively refers to abnormalities of insulin metabolism that include HI and insulin resistance (IR) [6]. Potential causes of HI include enhanced islet capacity under metabolic demand and impaired insulin clearance (hepatic or peripheral) [7]. The widely accepted explanation for HI is that a decrease in tissue insulin sensitivity results in an increase in insulin secretion, causing HI and what is referred to as compensated IR [8]. The relationship between ID and concurrent endocrine disease such as pituitary pars intermedia dysfunction (PPID) has not been extensively explored but is relevant as horses that are co-affected with ID and PPID often have higher baseline insulin concentrations than horses with ID alone and thus are at a higher risk of laminitis [9].

* Corresponding author.
*E-mail address:* psvagerko@ufl.edu (P. Teague).

https://doi.org/10.1016/j.domaniend.2026.106998
Received 21 July 2025; Received in revised form 2 February 2026; Accepted 3 February 2026
Available online 4 February 2026

In other species, metabolic syndrome results in a prediabetic state that is followed by the development of Type 2 Diabetes (T2D) if there is no intervention. The disease T2D develops when beta-cells are unable to secrete sufficient amounts of insulin due to their dysfunction, damage, or death [10]. Horses rarely develop T2D but instead remain in a hyperinsulinemic and euglycemic compensatory state for a prolonged period. In both EMS horses and people with early-stage prediabetes, insulin concentrations are increased compared to healthy individuals [11,12]. In people, total beta-cell mass and functional capacity initially increase in response to IR, but both decline as diabetes progresses [13]. Results from Do and colleagues showed that prediabetic mice had an increase in islet size and insulin content, as well as a decrease in the relative percentage of alpha-cells [14]. They also looked at the functionality of the beta-cells in the prediabetic mice and found that there was an increase in exocytic events, suggesting an increase in beta-cell productivity (insulin release) during the prediabetic stage [14]. Investigating these topics in the horse may provide insight into the pathophysiology of equine ID.

To the author's knowledge, there is only one study that previously assessed islet area in horses with endocrine disease, which reported no difference in the mean relative islet area of pancreatic islets between insulin-sensitive and insulin-resistant horses. Additionally, they did not find an increase in insulin immunoreactivity in the pancreatic islets of insulin-resistant horses but did see a decrease in glucagon immunoreactivity. As this study only assessed ten islets per slide of pancreatic tissue in a total of ten insulin-resistant horses, a more thorough examination is necessary [4].

The mechanism by which horses with ID can maintain compensatory HI and resist beta-cell failure is unknown and identifying this mechanism may help prevent or manage the onset of laminitic episodes in horses. Additionally, understanding this could offer insights into preventing beta-cell failure in other species. First, a preliminary study using advanced image analysis methods was conducted to determine the anatomical distribution of islets within the equine pancreas and to explore islet composition across different locations. It was hypothesized that the islet area, perimeter, and endocrine cell composition would vary based on the anatomical location within the pancreas. Next, as a step towards understanding how horses respond to chronic insulin demand, islet morphology and composition were compared between normal and HI horses. It was hypothesized that 1) horses with HI have an increased pancreatic islet area and beta-cell mass compared to non-HI horses and 2) horses co-affected with HI and PPID have an increased pancreatic islet area and beta-cell mass compared to horses with HI alone. Finally, we sought to investigate how PPID influences pancreatic islet morphology and cellular composition. Together, this research aimed to contribute valuable insights into the normal structure and structural adaptions of the equine pancreas in disease.

## 2. Methodology

### Study 1: Distribution and Composition of Islets in the Normal Equine Pancreas

#### 2.1. Pancreas sampling

The pancreas was obtained from eight horses presenting for necropsy or disposal after being euthanized for reasons unrelated to this study. Only adult (4-15 years) light breed horses without clinical signs of EMS (BCS $< 7$, absence of regional adiposity or evidence of laminitis) or PPID were included. Each pancreas was collected immediately after euthanasia and fixed in 10% formalin for a minimum of 24 hours before trimming. Samples were taken from 25%, 50%, and 75% distances from the tips of both the left and right lobes of the pancreas and at three distinct points on the pancreatic body: left, center, and right, and then embedded in paraffin. Sections were cut from these samples in 2-4 mm blocks for subsequent staining and immunohistochemical analyses.

The obtained samples were processed and prepared with hematoxylin and eosin (H&E) stain or no stain by the University of Florida's College of Veterinary Medicine Diagnostic Laboratory, then digitized at 40X magnification for histologic examination using software for digital pathology and whole-slide image analysis[1] as well as quantitative image analysis[2]. Whole-slide image analysis was used to manually measure relative islet area by calculating the islet area relative to the pancreatic tissue area, as well as other individual islet characteristics across different regions of the pancreas. Quantitative analysis of immunostaining was performed using quantitative image analysis[2]. The software was trained using ten representative samples to differentiate islet from non-islet pancreatic tissue. Training was guided by a board-certified veterinary pathologist and refined using the software's assisted AI-based tissue classifier until accurate recognition of islets was achieved. After training, the algorithm was applied to all slides to quantify the immunostaining of insulin, glucagon, and somatostatin within each pancreatic tissue sample. Stain detection was performed with threshold values adjusted to match visually confirmed staining intensity and to exclude background signal. The software reported the positive stain per unit of pancreas as well as the average percentage of each hormone per islet in each region. Validation was performed by visually comparing automated segmentation and stain detection against expert annotations, and analysis proceeded once detection accuracy reached an acceptable range.

#### 2.2. Immunohistochemical analysis

Pancreatic tissue from each horse was collected as described above. For each horse, 3 serial pancreatic sections from each region were each stained with antibodies against insulin[3] (dilution 1:500), glucagon[4] (dilution 1:500), or somatostatin[5] (dilution 1:1000). Slides underwent deparaffinization in xylene, rehydration through graded ethanol, and quenching of endogenous peroxidase with 3% $H_2O_2$. Antigen retrieval was performed using citrate buffer. After blocking[6], slides were incubated with the primary antibody at 4°C for 24 hours. Following PBS washes, a biotinylated secondary antibody[7] and avidin-biotin complex (VECTASTAIN Elite ABC—HRP Kit (PK-6200))[8] were applied. Staining was developed using DAB substrate[9], and slides were dehydrated through graded ethanol and cleared in xylene. Coverslips were mounted using Eukitt quick-hardening mounting media[10] and allowed to dry completely. Finally, the slides were digitized at 40X magnification for histologic examination using software for digital pathology and whole-slide image analysis[1] as well as quantitative image analysis[2].

### Study 2: Pancreatic Islet Remodeling in Horses with Hyperinsulinemia and Pituitary Dysfunction

All testing protocols were approved by the Oklahoma State University Institutional Care and Use Committee.

[1] QuPATH: Open-source software for digital pathology image analysis.
[2] HALO Image Analysis Platform version 4.1.5944 and HALO AI version 4.1.5944 (Indica Labs, Inc.).
[3] Insulin antibody #4590, Cell Signaling Technology.
[4] Glucagon antibody, Product ID: 20076, ImmunoStar Inc, Hudson, WI.
[5] Somatostatin antibody, Product ID: 20067, ImmunoStar Inc, Hudson, WI.
[6] Citrate Buffer, pH 6.0, 10x, Antigen Retriever, Sigma Aldrich.
[7] Normal Goat Serum Blocking Solution (S-1000-20), Vector Laboratories.
[8] Goat Anti-Rabbit IgG Antibody ($H + L$), Biotinylated (BA-1000-1.5), Vector Laboratories.
[9] DAB Substrate Kit, Peroxidase (HRP), with Nickel (3,3′-diaminobenzidine) (SK-4100), Vector Laboratories Inc.
[10] Eukitt Quick-hardening mounting medium, Sigma Aldrich.

### 2.3. Animals

Horses included in this study were assigned to one of four groups based on retrospective evaluation of clinical records, phenotypic characteristics, endocrine testing, and histopathologic findings. Control horses were over two years of age, had a body condition score (BCS) $\leq$ 6/9, no history of laminitis, and were considered normoinsulinemic based on a baseline serum insulin concentration $<$ 20 μIU/mL [15]. These horses showed no clinical signs of PPID and had a pituitary histopathology score $\leq$ 3/5 [16]. Horses classified as EMS demonstrated a BCS $>$ 6/9 with regional adiposity and underwent prior dynamic testing which resulted in baseline insulin concentrations $>$ 20 μIU/mL and/or post-oral sugar test insulin concentration $>$ 45 μIU/mL. An insulin sample was collected at euthanasia, and horses were considered hyperinsulinemic if insulin concentrations were $>$ 20 μIU/mL and non-hyperinsulinemic if insulin concentrations were $<$ 20 μIU/mL. Horses with PPID were diagnosed based on the presence of clinical signs, including hypertrichosis and muscle wasting, along with a pituitary histopathology score $\geq$ 4/5 [16]. Horses co-affected exhibited both EMS phenotype and PPID diagnostic criteria. In cases where pituitary samples were unavailable ($n = 2$), diagnosis of PPID was supported by the presence of clinical signs, a non-autumn plasma ACTH $>$ 35 pg/ml, and a positive dexamethasone suppression test.

### 2.4. Blood sampling and analysis

Blood samples were collected at the time of euthanasia and plasma and serum frozen at −80°C until time of analysis. Plasma ACTH was measured by chemiluminescent assay (Immulite 1000, Siemens) at Oklahoma State University's College of Veterinary Medicine. Serum samples were sent for insulin analysis via radioimmunoassay at the Animal Health Diagnostic Center at Cornell University's College of Veterinary Medicine.

### 2.5. Pancreatic sampling and immunohistochemical analysis

Pancreatic tissue samples were processed, embedded in paraffin, and stained with H&E or unstained for subsequent immunohistochemical analysis for insulin, glucagon, and somatostatin as described in Study 1.

### 2.6. Statistical analysis

The normality of the data was assessed using the Shapiro-Wilk test. For normally distributed variables, the mean ± standard deviation was reported. For non-normally distributed variables, the median [interquartile range, IQR] was reported.

In the preliminary study, an analysis of variance (ANOVA) was used to analyze relative islet area, individual islet area, and islet perimeter in each sampling location across the lobes and the composition of islets in terms of insulin, glucagon, and somatostatin in separate analyses for each hormone. Each horse contributed nine predefined sampling locations, which were analyzed using a repeated-measures ANOVA, with horse as the subject and sampling location as the within-subject factor.

In the second study, the relative islet area (islet area relative to pancreatic tissue area), individual islet area, islet perimeter, shape index, and islet count from the left lobe were first compared between non-HI and HI and between non-PPID and PPID horses using an unpaired t-test. All horses were then grouped more specifically: control, EMS, PPID, or EMS+PPID. Those groups were compared using a one-way ANOVA. Disease group was treated as the fixed effect and Tukey's HSD was conducted to explore significant differences between the groups. Differences in BCS among the four disease groups were assessed using a Kruskal-Wallis test, followed by Dunn's multiple comparisons test for post-hoc pairwise comparisons.

The shape of islets was assessed using a shape index (also referred to as circularity) to evaluate the degree of roundness or irregularity. Shape index was calculated using the following formula: Shape Index = $(4\pi \times \text{Area}) / (\text{Perimeter})^2$ where area represents the total cross-sectional area of the islet ($\mu m^2$) and perimeter represents the total outline length of the islet (μm). Measurements of islet area and perimeter were obtained using whole-slide image analysis software[1]. For each tissue section, the shape index values of all individual islets were averaged to generate a mean shape index per sample for statistical analysis. A shape index value of 1.0 corresponds to a perfect circle, while lower values indicate increasing irregularity or elongation of the islet structure.

The immunoreactivity of insulin, glucagon, and somatostatin and percentage of hormone per islet were analyzed separately between non-HI and HI and between non-PPID and PPID using an unpaired t-test, and across the four disease groups using a one-way ANOVA. For each hormone, disease group was treated as a fixed effect and Tukey's HSD was conducted to explore significant differences between the groups.

All statistical analyses were performed using GraphPad Prism (version 10.4.2; GraphPad Inc). Statistical significance was defined as $p < 0.05$.

## 3. Results

**Study 1**

### 3.1. Relative islet area

Mean relative islet area did not differ within each lobe ($p > 0.05$) but differed at certain sampling locations among lobes. The sampling locations as 25% and 75% from the tip of the left lobe had a greater relative islet area than all sampling locations in the body and right lobe ($p < 0.01$). Mean relative islet area was overall greater in the left lobe (0.02 ± 0.003) than both the body (0.01 ± 0.004) and right lobe (0.01 ± 0.005; $p < 0.001$; Fig. 1A).

### 3.2. Individual islet area

Mean individual islet area did not differ across any sampling locations nor overall across the left lobe (10680.33 ± 1586.18 $\mu m^2$), body (10946.92 ± 2 284.16 $\mu m^2$), or right lobe (10757.04±2141.64 $\mu m^2$) of the pancreas ($p > 0.05$).

### 3.3. Islet perimeter

Mean islet perimeter did not differ within each lobe ($p > 0.05$) but differed at certain sampling locations between lobes. All sampling locations in the left lobe were greater than all sampling locations in the body and right lobe ($p < 0.01$). Mean individual islet perimeter was overall greater in the left lobe (397 ± 67 μm) than both the body (274 ± 46 μm) and right lobe (263 ± 49 μm; $p < 0.001$; Fig. 1B).

### 3.4. Hormone immunostaining in pancreatic islets

There were no differences in total area of hormone immunostaining of insulin, glucagon, or somatostatin per unit of pancreas across all sampling locations ($p > 0.05$). Additionally, the mean percentage of beta-cells (54.9 ± 17.9%), alpha-cells (28.7 ± 4.9%), or delta-cells cells (15.2 ± 9.7%) within islets did not differ across sampling locations ($p > 0.05$). Islets had an alpha-cell core and a beta-cell mantle with delta-cells randomly dispersed (Fig. 2).

**Study 2**

### 3.5. Animals

A total of 35 animals were included in this study: 13 in the control group, 8 in the EMS group, 9 in the PPID group, and 5 in the EMS+PPID

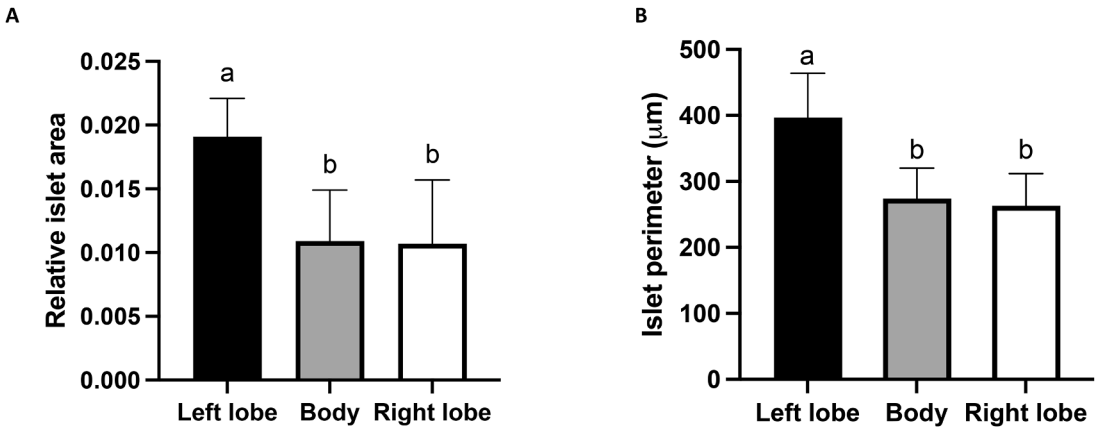


**Fig. 1.** (A) Mean relative islet area in the left lobe, body, and right lobe of the equine pancreas of eight horses. (B) Mean islet perimeter in the left lobe, body, and right lobe of the equine pancreas of eight horses. Differing letters denote $p < 0.001$.

group (Table 1). Groups were similar in breed type and sex distribution. As expected, the PPID group was significantly older than both the control and EMS groups. Body condition score was higher in both EMS and EMS+PPID groups compared to the control and PPID groups.

Within the EMS group, 6 horses had a baseline serum insulin > 20 μIU/mL at the time of euthanasia and were therefore classified as HI. The 2 horses (QHs, BCS 8 and 9, 13 years) in the EMS group that had a baseline serum insulin concentration < 20 μIU/ml at euthanasia had previously tested positive for ID based on results from an oral sugar test (OST). One of the two horses also had a history of laminitis. All EMS+PPID horses were hyperinsulinemic.

### 3.6. Pancreatic islet morphology and hormone composition across disease groups

#### 3.6.1. Relative islet area

Mean relative islet area was >2-fold greater in the HI (0.0158 ± 0.007) compared to the non-HI group (0.0075 ± 0.005; $p < 0.001$; Fig. 3A). There was no difference in mean relative islet area between the non-PPID (0.0098 ± 0.006) and PPID groups (0.0134 ± 0.009; $p > 0.05$; Fig. 3B). When comparing across the four disease groups, the EMS (0.016 ± 0.002) and EMS+PPID (0.0183 ± 0.008) had significantly greater mean relative islet area than the control group (0.0059 ± 0.004; $p < 0.001$; Fig. 3C). Horses with EMS+PPID had a significantly greater mean relative islet area than horses with PPID alone (0.0094 ± 0.006; $p < 0.05$). There were no differences in mean relative islet area between the control and PPID nor between EMS and PPID groups ($p > 0.05$).

#### 3.6.2. Individual islet area

Mean individual islet area was 1.6-fold greater in the HI (5798 ± 2624 μm$^2$) compared to the non-HI group (9559 ± 4136 μm$^2$; $p < 0.01$; Fig. 4A). There was no difference in mean individual islet area between non-PPID (6509 ± 2994 μm$^2$) and PPID groups (8223 ± 4485 μm$^2$; $p > 0.05$; Fig. 4B). Across the four disease groups, the EMS (8983 ± 2907 μm$^2$) and EMS+PPID (10480 ± 5901 μm$^2$) had significantly greater mean individual islet area compared to the control group (4987 ± 1848 μm$^2$; $p < 0.05$; Fig. 4C). The control and PPID groups (6970 ± 3214 μm$^2$) did not differ, nor did the EMS and EMS+PPID groups ($p > 0.05$).

### 3.7. Islet perimeter

Mean islet perimeter was greater in the HI (434.8 ± 226.1 μm) compared to the non-HI group by almost 1.5-fold (298.9 ± 133.4 μm; $p < 0.05$). There was no difference in mean islet perimeter between non-PPID (320.1 ± 180.4 μm) and PPID groups (393.2 ± 184.5 μm; $p > 0.05$). There was no difference in mean islet perimeter across control (250.3 ± 50.92 μm), EMS (433.5 ± 254.5 μm), PPID (369.1 ± 182.9 μm), and EMS+PPID groups (436.7 ± 200.1 μm; $p = 0.0729$).

### 3.8. Shape index

Shape index did not differ between non-HI (0.55 ± 0.15) and HI (0.49 ± 0.19), between non-PPID (0.52 ± 0.12) and PPID (0.54 ± 0.22), nor across control (0.54 ± 0.11), EMS (0.48 ± 0.13), PPID (0.56 ± 0.20), and EMS+PPID groups (0.50 ± 0.27; $p > 0.05$).

### 3.9. Islet count

Mean islet count did not differ between non-HI (320 ± 136) and HI groups (302 ± 192; $p > 0.05$; Fig. 5A). The PPID group (406 ± 128) had a greater mean islet count than the non-PPID group (251 ± 145; $p < 0.01$; Fig. 5B). Mean islet count also differed across control (256 ± 117), EMS (180 ± 73), PPID (412 ± 109), and EMS+PPID groups (395 ± 171; $p < 0.01$; Fig. 5C), with the PPID group having a greater islet count than the control group ($p < 0.05$). Neither the EMS nor the EMS+PPID groups were different than the control group ($p > 0.05$), however, the EMS group had a lower islet count than both the PPID and EMS+PPID groups ($p < 0.05$). The control and EMS groups did not differ ($p > 0.05$).

### 3.10. Hormone immunoreactivity per unit of pancreas

As anticipated, insulin immunoreactivity per unit of pancreas followed the same pattern as the islet area per unit of pancreas (Figs. 3D-F). The HI (0.0202 ± 0.009) had greater insulin immunoreactivity per unit of pancreas compared to the non-HI group (0.0135 ± 0.008; $p < 0.05$; Fig. 3D). Non-PPID (0.0098 ± 0.006) and PPID groups (0.0134 ± 0.009) showed no difference in insulin immunoreactivity per unit of pancreas ($p > 0.05$; Fig. 3E). When comparing across control (0.0059 ± 0.004), EMS (0.0161 ± 0.003), PPID (0.0099 ± 0.006), and EMS+PPID (0.0198 ± 0.009), there were significant differences ($p < 0.0001$; Fig. 3F). Both EMS and EMS+PPID groups had greater insulin immunoreactivity than the control group ($p < 0.01$). There was no difference between control and PPID groups ($p > 0.05$), nor between EMS and EMS+PPID groups ($p > 0.05$).

Glucagon immunoreactivity per unit of pancreas did not differ between non-HI (0.0084 [0.0033-0.0193]) and HI groups (0.0086 [0.0026-0.0144]), between non-PPID (0.0097 [0.0039-0.0144]) and PPID groups (0.004 [0.0031-0.0201]), nor across control (0.0097 [0.0039-0.0356]), EMS (0.0091 [0.0027-0.0135]), PPID (0.0044 [0.0028-0.0152]), and EMS+PPID groups (0.0035 [0.0026-0.1628]; $p > 0.05$).

Somatostatin immunoreactivity per unit of pancreas did not differ

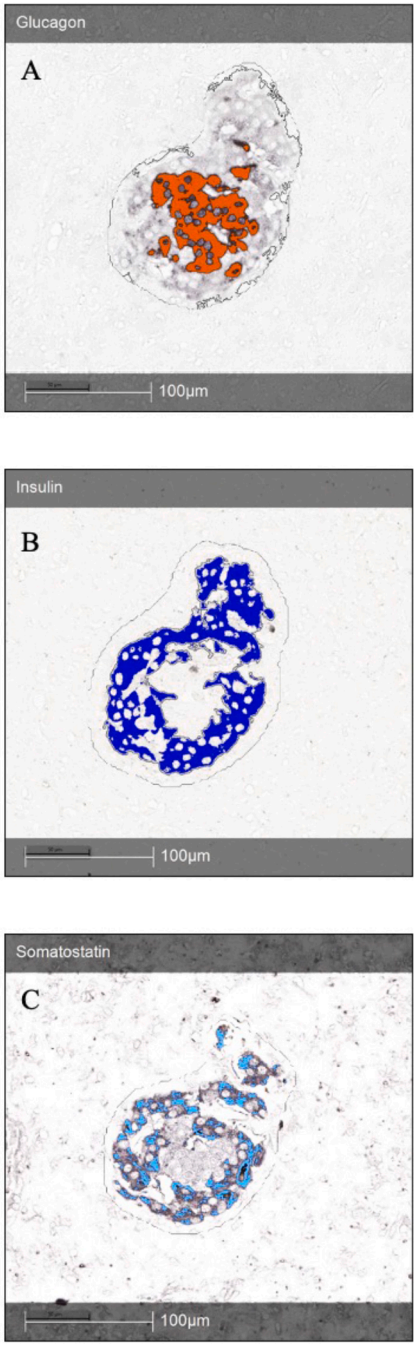


**Fig. 2.** Serial pancreatic sections that were immunohistochemically stained for glucagon (A), insulin (B), and somatostatin (C) within the islets after an intuitive image analysis program was used to change the brown chromogen with hormone-expressing cells to a certain color per hormone to quantify immunostaining.

between non-HI (0.047 ± 0.037) and HI (0.0353 ± 0.019) groups, between non-PPID (0.0448 ± 0.037) and PPID (0.0396 ± 0.021) groups, nor across control (0.0511 ± 0.044), EMS (0.0344 ± 0.019), PPID (0.0412 ± 0.023), and EMS+PPID (0.0368 ± 0.02) groups ($p > 0.05$).

### 3.11. Percentage of hormone immunoreactivity per islet

Percentage of insulin immunoreactivity per islet were similar between non-HI (55.94 ± 7.98%) and HI (50.22 ± 9.63%) groups ($p = 0.06$), and between the non-PPID (51.76 ± 10.22%) and PPID (56.9 ± 5.58%) groups ($p = 0.09$). The difference in percentage of insulin immunoreactivity per islet was also similar across control (54.72 ± 9.32%), EMS (46.95 ± 10.34%), PPID (57.7 ± 5.57%), and EMS+PPID groups (55.46 ± 5.92%; $p = 0.07$).

Percentage of glucagon immunoreactivity per islet did not differ between non-HI (26.32 ± 12.07%) and HI (28.54 ± 9.21%) groups, between non-PPID (26.34 ± 11.32) and PPID (28.36 ± 10.83) groups, nor across control (23.92 ± 12.01%), EMS (30.26 ± 9.5%), PPID (29.79 ± 11.97%), and EMS+PPID (25.78 ± 9.02%) groups ($p > 0.05$).

Percentage of somatostatin immunoreactivity per islet did not differ between non-HI (16.83 ± 8.53%) and HI (13.16 ± 8.66%) groups, between non-PPID (17.05 ± 9.82%) and PPID (13.08 ± 6.07%) groups, nor across control (18.96 ± 9.72%), EMS (13.95 ± 9.78%), PPID (13.74 ± 5.59%), and EMS+PPID (11.89 ± 7.39%) groups ($p > 0.05$).

**Table 1**
Signalment, baseline insulin, and ACTH concentrations in control (CON), EMS, PPID, and EMS+PPID horses; age, body condition score (BCS), baseline insulin concentration, and baseline ACTH concentration are presented as mean ± standard deviation. Abbreviations: ST (stock type), LB (light breed), PB (pony breed), DB (draft breed); M (mare), G (gelding), S (stallion).

| | CON ($n = 13$) | EMS ($n = 8$) | PPID ($n = 9$) | EMS+PPID ($n = 5$) | p-value |
|---|---|---|---|---|---|
| Breed | 10 ST, 2 LB | 3 ST, 4 LB, 1 PB | 8 ST, 1 LB | 4 LB, 1 PB | 0.3729 |
| Gender | 10 M, 3 G | 4 M, 4 G | 5 M, 4 G | 4 M, 1 G | 0.4755 |
| Age (years) | 19.1 ± 7.4[a] | 12.9 ± 3.3[a] | 27 ± 6.1[b] | 18.6 ± 3[ab] | **0.0003** |
| BCS | 5 [4.5-5][a] | 8 [8-9][b] | 3 [2-4][a] | 7 [7-9][b] | **<0.0001** |
| Insulin (µIU/ml) | 28.8 ± 16.2[a] | 242.6 ± 270.9[b] | 25.6 ± 9.4[a] | 330.5 ± 276.8[b] | **0.0014** |
| ACTH (pg/ml) | 58.8 ± 62.5[a] | 44.4 ± 19.9[a] | 486.1 ± 411[b] | 353.1 ± 206.5[ab] | **0.0003** |

## 4. Discussion

In the normal equine pancreas, differences in islet characteristics may reflect structural or functional variability. The greater mean relative islet area and individual islet perimeter in the left lobe suggest a higher islet density compared to the body and right lobe, possibly indicating regional specialization. A larger islet perimeter without a proportional increase in individual area implies more irregular or elongated islet shapes in the left lobe. These differences may stem from regional variation in blood flow or innervation [17,18]. Embryological origins may also contribute to structural and functional differences. In horses, the pancreas arises from two embryonic buds: the dorsal bud gives rise to the left lobe and part of the body, and the ventral bud forms the right lobe and the head [3,19]. Tissues derived from the dorsal bud are more vascularized and may show greater endocrine activity, aligning with the increased islet area and perimeter observed in the left lobe [20,21]. This could reflect a developmental basis for the left lobe's potential role in postprandial glucose regulation.

Equine islet architecture, first described in the 1970′s [2], has been confirmed by later studies [3,4], all showing an alpha-cell core, beta-cell mantle, and randomly dispersed delta-cells. While islet composition has only been assessed by anatomical location once before, both that study and the present one found similar percentages of insulin, glucagon, and somatostatin across the pancreas [3]. The current study additionally quantified total immunostaining area relative to pancreatic tissue area and found uniform expression across lobes.

Islets were composed of approximately 54.9% insulin-producing cells, 28.7% glucagon-producing cells, and 15.2% somatostatin-producing cells, closely matching prior data [3,4]. Islet structure and cell composition vary widely across species. Rodents and dogs have a beta-cell core with alpha- and delta-cell peripheries, while humans and cats exhibit a more mixed cell arrangement. Livestock typically have a

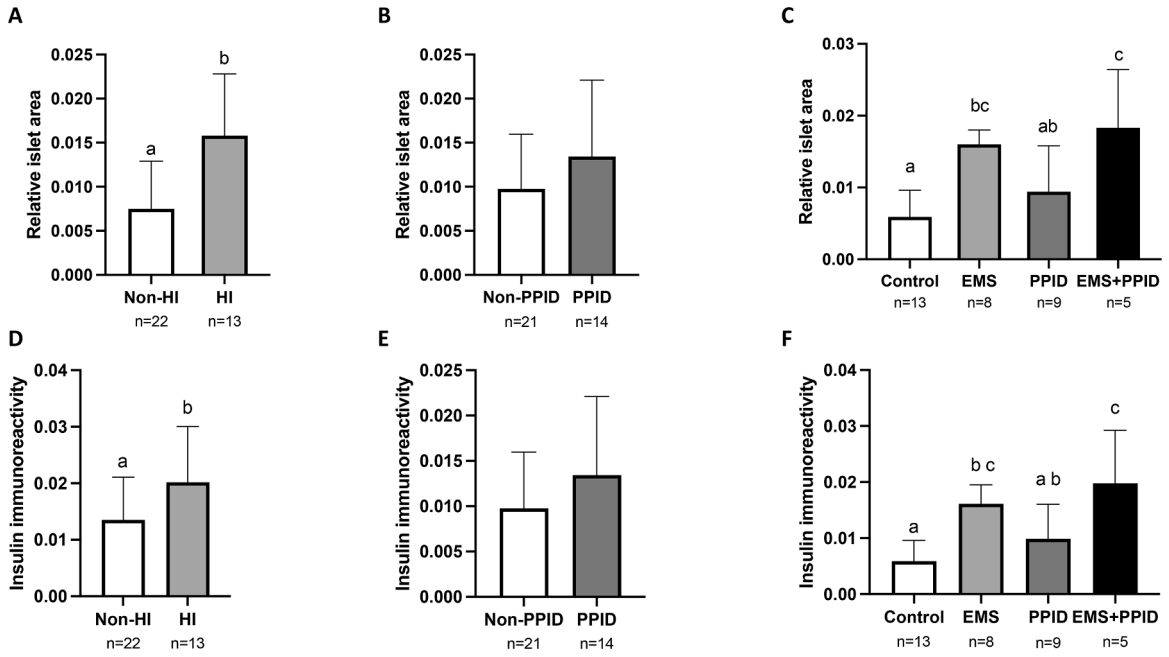


**Fig. 3.** (A) Mean relative islet area for non-HI and HI groups. (B) Mean relative islet area for non-PPID and PPID groups. (C) Mean relative islet area for control, EMS, PPID, and EMS+PPID groups. (D) Mean insulin immunoreactivity per unit of pancreas for non-HI and HI groups. (E) Mean insulin immunoreactivity per unit of pancreas for non-PPID and PPID groups. (F) Mean insulin immunoreactivity per unit of pancreas of control, EMS, PPID, and EMS+PPID groups. Differing letters denote $p < 0.01$.

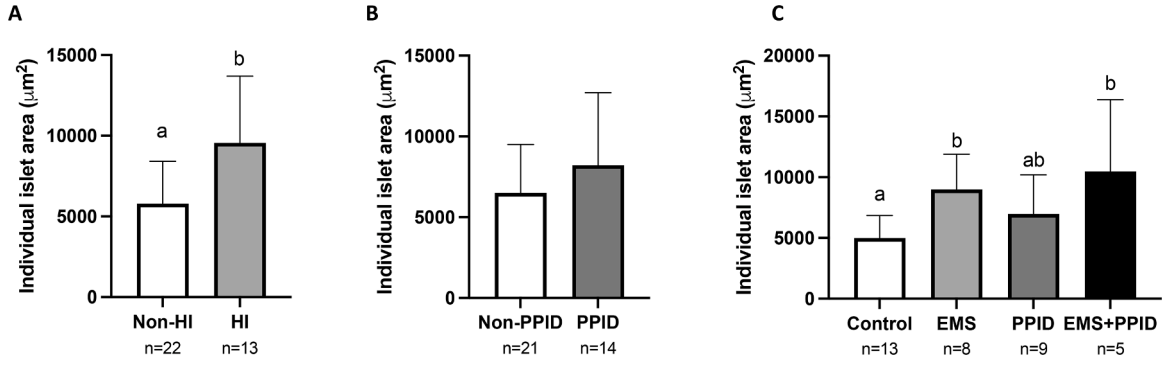


**Fig. 4.** (A) Mean individual islet area for non-HI and HI groups. (B) Mean individual islet area for non-PPID and PPID groups. (C) Mean individual islet area for control, EMS, PPID, and EMS+PPID groups. Differing letters denote $p < 0.05$.

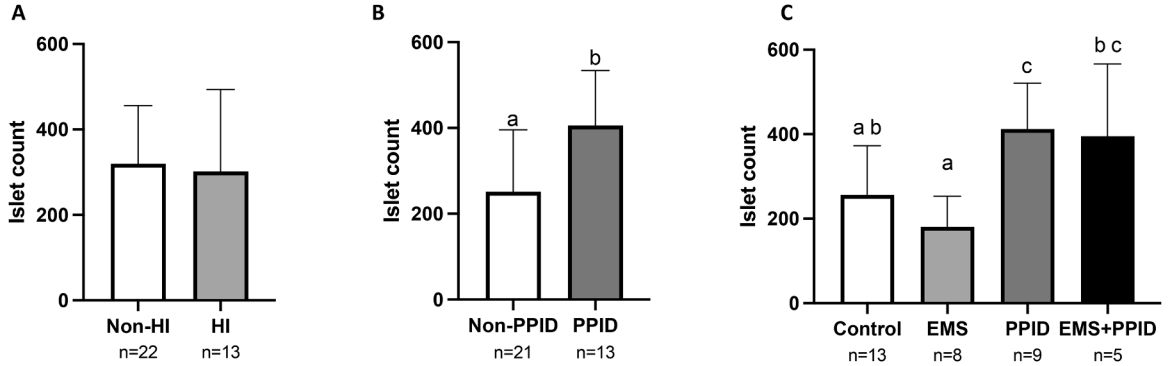


**Fig. 5.** (A) Mean islet count for non-HI and HI groups. (B) Mean islet count for non-PPID and PPID groups. (C) Mean islet count for control, EMS, PPID, and EMS+PPID groups. Differing letters denote $p < 0.05$.

beta-cell core and alpha-cell mantle, though frequencies are poorly documented. Notably, only certain nonhuman primates share the horse's alpha-cell core, beta-cell mantle organization, though their cell frequencies differ with 60-90% beta-cells, 20% alpha-cells, and 5%

delta-cells [22].

A key finding of this study was that hyperinsulinemia is primarily associated with islet enlargement and increased beta-cell mass, whereas PPID appears to be linked to increased islet numbers with no change in islet size or beta-cell mass. The observed relationship between hyperinsulinemia and islet enlargement is consistent with findings in other species, where prolonged insulin resistance (IR) drives islet expansion, allowing for maintenance of glucose homeostasis in the face of IR [13]. In contrast, previous reports examining equine islets found no difference in islet area in horses with insulin dysregulation (ID) [4]. However, the current study evaluated almost 30-fold more islets using more sophisticated technology to quantify islet area. There was no difference in relative islet area between PPID and control horses, suggesting that PPID alone does not contribute to significant islet enlargement. This is further supported by the individual islet area findings, where EMS and EMS+PPID horses had significantly larger islets than control horses, whereas PPID horses did not differ from controls.

Islet perimeter followed a similar pattern, with HI horses having greater perimeter measurements than non-HI horses, reinforcing that islet size increases in the presence of HI. Unlike islet area and perimeter, islet shape index did not differ across disease groups, indicating that despite changes in size, the overall morphology of islets remained consistent.

A particularly interesting finding was the significant increase in islet count in PPID horses compared to non-PPID horses. This suggests that PPID may promote islet proliferation, possibly through chronic endocrine stimulation. While HI appears to be associated with fewer but larger islets, PPID appears to drive an overall increase in islet number, suggesting different mechanisms of islet adaptation to chronic increased metabolic demands. The reasons for this difference remain unclear but could be linked to distinct hormonal influences on pancreatic remodeling. During embryogenesis, islet cells originate from primitive duct-like cells, and postnatally, pancreatic endocrine mass expands through either beta-cell proliferation or islet neogenesis. While beta-cell replication is well established, the idea that ductal cells continue to generate new beta-cells remains debated [23]. Recent studies have demonstrated that pancreatic ductal cells expressing Neurogenin3 (Ngn3) can differentiate into beta-cells under certain conditions. For instance, research in mice has shown that Ngn3-expressing ductal cells contribute to beta-cell neogenesis during both homeostatic and diabetic states [24]. In aged horses, neogenesis of endocrine cells and islet hyperplasia have been observed in close association with the pancreatic duct, indicating a process termed nesidioblastosis [25]. Given that PPID horses were significantly older than non-PPID horses, age was initially considered as a potential confounding factor. However, correlation analyses (data not shown) within each group did not reveal a relationship between age and islet number, suggesting that the observed increase in islet count is unlikely to be solely attributable to age. In horses with PPID, the increased number of smaller islets suggests ongoing neogenesis, which may be driven by hormonal imbalances characteristic of the disease, particularly elevated alpha-MSH, which has been shown to exert trophic and anti-inflammatory effects on endocrine tissues [26,27]. Investigating Ngn3 expression and ductal markers in the pancreas of PPID-affected horses and assessing how ductal cells respond to these altered hormone concentrations could elucidate a previously unreported mechanism of islet neogenesis in the horse.

The analysis of hormone immunoreactivity per unit of pancreas further supports the role of HI in pancreatic adaptation. HI horses exhibited greater insulin immunoreactivity than non-HI horses, suggesting increased beta-cell capacity, while there was no difference between PPID and non-PPID horses, reinforcing the idea that PPID alone does not drive increased pancreatic insulin production. In contrast, glucagon and somatostatin immunoreactivity did not differ between groups, suggesting that while HI affects beta-cell function, alpha- and delta-cell populations remain relatively stable in these horses.

While these findings provide valuable insights into pancreatic islet adaptations in horses with endocrine disease, several limitations should be considered. Ideally, all horses included in the EMS group would have been hyperinsulinemic. In fact, when originally screened prior to this study using different assays, all were classified as insulin dysregulated based on baseline or dynamic testing. However, at the time of enrollment two horses failed to meet the diagnostic thresholds despite both having a BCS $\geq$ 8/9 and one having extensive history of pasture-associated laminitis. This highlights a known limitation of relying on single time point measurements, as baseline insulin concentrations may yield false negatives, particularly in cases of mild or early insulin dysregulation [28]. It is unknown if the variation in diagnostic outcome is a result of lack of repeatability of insulin testing in horses, differences in insulin assays, or other laboratory related issues [29]. For PPID classification, pituitary samples were not available for 6 horses; however, these horses were categorized based on clinical signs, positive dexamethasone suppression test results, and elevated non-fall ACTH concentrations, which are widely accepted diagnostic markers. Breed variation was also present in the study population, with a mix of ponies, light horse breeds, and stock horse breeds, which may have an influence on islet morphology and hormone immunoreactivity. The small sample size for each breed precludes drawing any conclusions regarding breed influences in this study. Lastly, the overall sample size per group was a limitation of the study. Despite these limitations, the current findings provide meaningful contributions to our understanding of pancreatic adaptations in equine metabolic and endocrine disease and suggest the need for further studies.

In conclusion, this study advances our understanding of the normal equine endocrine pancreas as well as the impact of HI and PPID, highlighting distinct patterns of islet remodeling in response to metabolic and pituitary-derived stimuli. The divergence between islet enlargement in HI and increased islet count in PPID supports the concept of disease-specific mechanisms of pancreatic adaptation. These findings not only add to the limited body of literature on equine pancreatic physiology but also suggest avenues for further investigation, particularly into the role of ductal-cell derived neogenesis and the impact of pituitary-derived hormones on islet health. Continued research in this area is essential to fully characterize the mechanisms underlying endocrine pancreas plasticity in horses and to explore potential therapeutic targets for metabolic and pituitary disorders in this species.

## CRediT authorship contribution statement

**P. Teague:** Writing – review & editing, Writing – original draft, Visualization, Validation, Software, Project administration, Methodology, Investigation, Formal analysis, Data curation, Conceptualization. **M. Dark:** Writing – review & editing, Software, Methodology, Data curation. **D. Verdugo:** Software, Data curation. **D. Freeman:** Resources. **D. McFarlane:** Writing – review & editing, Writing – original draft, Visualization, Supervision, Resources, Project administration, Methodology, Investigation, Funding acquisition, Conceptualization.

## Acknowledgements

The author would like to thank Dr. Nicholas Frank (Mississippi State University College of Veterinary Medicine, 240 Wise Center Drive, Starkville, Mississippi, United States) for providing samples used in this research.

## References

[1] Forssmann A. The ultrastructure of the cell types in the endocrine pancreas of the horse. Cell Tissue Res 1976;167:179–95. https://doi.org/10.1007/BF00224326.
[2] Helmstaedter V, Feurle G, Forssmann WG. Insulin, glucagon-, and somatostatin-immunoreactive endocrine cells in the equine pancreas. Cell Tissue Res 1976;172:447–54. https://doi.org/10.1007/BF00220331.

[3] Furuoka H, Ito H, Hamada M. Immunocytochemical component of endocrine cells in pancreatic islets of horses. Jpn J Vet Sci 1989;51:35–43. https://doi.org/10.1292/jvms1939.51.35.
[4] Newkirk KM, Ehrensing G, Odoi A, Boston RC, Frank N. Immunohistochemical expression of insulin, glucagon, and somatostatin in pancreatic islets of horses with and without insulin resistance. Am J Vet Res 2018;79:191–8. https://doi.org/10.2460/ajvr.79.2.191.
[5] Frank N, Geor Rj, Bailey Sr, Durham Ae, Johnson Pj. Equine metabolic syndrome. J Vet Intern Med 2010;24:467–75. https://doi.org/10.1111/j.1939-1676.2010.0503.x.
[6] Frank N, Tadros EM. Insulin dysregulation. Equine Vet J 2014;46:103–12. https://doi.org/10.1111/evj.12169.
[7] Mudaliar S, Henry RR. Effects of incretin hormones on β-cell mass and function, body weight, and hepatic and myocardial function. Am J Med 2010;123:S19–27. https://doi.org/10.1016/j.amjmed.2009.12.006. Current Issues in the Treatment of Type 2 Diabetes.
[8] Treiber K, Kronfeld D, Hess T, Boston R, Harris P. Use of proxies and reference quintiles obtained from minimal model analysis for determination of insulin sensitivity and pancreatic beta-cell responsiveness in horses. Am J Vet Res 2006;66:2114–21. https://doi.org/10.2460/ajvr.2005.66.2114.
[9] de Laat MA, Sillence MN, Reiche DB. Phenotypic, hormonal, and clinical characteristics of equine endocrinopathic laminitis. J Vet Intern Med 2019;33:1456–63. https://doi.org/10.1111/jvim.15419.
[10] Dludla PV, Mabhida SE, Ziqubu K, Nkambule BB, Mazibuko-Mbeje SE, Hanser S, Basson AK, Pheiffer C, Kengne AP. Pancreatic β-cell dysfunction in type 2 diabetes: implications of inflammation and oxidative stress. World J Diabetes 2023;14:130–46. https://doi.org/10.4239/wjd.v14.i3.130.
[11] Reaven GM, Hollenbeck CB, Chen Y-DI. Relationship between glucose tolerance, insulin secretion, and insulin action in non-obese individuals with varying degrees of glucose tolerance. Diabetologia 1989;32:52–5. https://doi.org/10.1007/BF00265404.
[12] Tripathy D, Carlsson M, Almgren P, Isomaa B, Taskinen M-R, Tuomi T, Groop L. Insulin secretion and insulin sensitivity in relation to glucose tolerance: lessons from the Botnia Study. Diabetes 2000;49:975–80. https://doi.org/10.2337/diabetes.49.6.975.
[13] Weir GC, Bonner-Weir S. Five stages of evolving beta-cell dysfunction during progression to diabetes. Diabetes 2004;53:S16–21. https://doi.org/10.2337/diabetes.53.suppl_3.S16.
[14] Do OH, Gunton JE, Gaisano HY, Thorn P. Changes in beta cell function occur in prediabetes and early disease in the Leprdbmouse model of diabetes. Diabetologia 2016;59:1222–30. https://doi.org/10.1007/s00125-016-3942-3.
[15] Dunbar Lk, Mielnicki Ka, Dembek Ka, Toribio Re, Burns Ta. Evaluation of four diagnostic tests for insulin dysregulation in adult light-breed horses. J Vet Intern Med 2016;30:885–91. https://doi.org/10.1111/jvim.13934.
[16] Miller MA, Pardo ID, Jackson LP, Moore GE, Sojka JE. Correlation of pituitary histomorphometry with adrenocorticotrophic hormone response to domperidone administration in the diagnosis of equine pituitary Pars intermedia dysfunction. Vet Pathol 2008;45:26–38. https://doi.org/10.1354/vp.45-1-26.
[17] Hampton RF, Jimenez-Gonzalez M, Stanley SA. Unravelling innervation of pancreatic islets. Diabetologia 2022;65:1069–84. https://doi.org/10.1007/s00125-022-05691-9.
[18] Menger MD, Vajkoczy P, Beger C, Messmer K. Orientation of microvascular blood flow in pancreatic islet isografts. J Clin Invest 1994;93:2280–5. https://doi.org/10.1172/JCI117228.
[19] Slack J. Developmental biology of the pancreas Development. The Company of Biologists; 1995. https://doi.org/10.1242/dev.121.6.1569. |.
[20] Herrera P. Adult insulin- and glucagon-producing cells differentiate from two independent cell lineages | development. The Company of Biologists; 2000. https://doi.org/10.1242/dev.127.11.2317. |.
[21] Pictet R. Development of the embryonic endocrine pancreas. Handb Physiol Sect 1972;7(1):25–66.
[22] Steiner, D.J., Kim, A., 2010. Pancreatic islet plasticity: interspecies comparison of islet architecture and composition. https://doi.org/10.4161/isl.2.3.11815.
[23] Rosenberg L. In vivo cell transformation: neogenesis of beta cells from pancreatic ductal cells. Cell Transpl 1995;4:371–83. https://doi.org/10.1016/0963-6897(95)00020-X. Plenary Lectures of the Second International Congress of the Cell Transplant Society.
[24] Gribben C, Lambert C, Messal HA, Hubber E-L, Rackham C, Evans I, Heimberg H, Jones P, Sancho R, Behrens A. Ductal Ngn3-expressing progenitors contribute to adult β cell neogenesis in the pancreas. Cell Stem Cell 2021;28:2000–8. https://doi.org/10.1016/j.stem.2021.08.003. e4.
[25] Furuoka H, Shirakawa T, Taniyama H, Ohishi H, Satoh H, Itakura C. Histogenesis of neoformation in the endocrine pancreas of aging horses. Vet Pathol 1989;26:40–6. https://doi.org/10.1177/030098588902600107.
[26] Brzoska T, Luger TA, Maaser C, Abels C, Böhm M. α-melanocyte-stimulating hormone and related tripeptides: biochemistry, antiinflammatory and protective effects in vitro and in vivo, and future perspectives for the treatment of immune-mediated inflammatory diseases. Endocr Rev 2008;29:581–602. https://doi.org/10.1210/er.2007-0027.
[27] Mazzocchi G, Rebuffat P, Robba C, Nussdorfer GG. Long-term trophic action of alpha-melanocyte-stimulating hormone on the zona glomerulosa of dexamethasone -or captopril-treated rats, with or without maintenance doses of ACTH or angiotensin. II: stereology and plasma hormone concentrations. Vivo Athens Greece 1987;1:31–4.
[28] Bertin FR, de Laat MA. The diagnosis of equine insulin dysregulation. Equine Vet J 2017;49:570–6. https://doi.org/10.1111/evj.12703.
[29] Karikoski NP, Box JR, Mykkänen AK, Kotiranta VV, Raekallio MR. Variation in insulin response to oral sugar test in a cohort of horses throughout the year and evaluation of risk factors for insulin dysregulation. Equine Vet J 2022;54:905–13. https://doi.org/10.1111/evj.13529.